ISSN 1063-7842, Technical Physics, 2007, Vol. 52, No. 4, pp. 401–408. © Pleiades Publishing, Ltd., 2007.
Original Russian Text © A.Yu. Jalnine, S.P. Kuznetsov, 2007, published in Zhurnal Tekhnicheskoĭ Fiziki, 2007, Vol. 77, No. 4, pp. 10–18.

THEORETICAL AND MATHEMATICAL PHYSICS

On the Realization of the Hunt–Ott Strange Nonchaotic Attractor in a Physical System

A. Yu. Jalnine and S. P. Kuznetsov

Institute of Radio Engineering and Electronics (Saratov Branch), Russian Academy of Sciences, ul. Zelenaya 38, Saratov, 410019 Russia

e-mail: spkuz@rambler.ru

Received June 19, 2006

Abstract—The object of investigation is a system consisting of two coupled nonautonomous van der Pol oscillators the characteristics frequencies of which differ by a factor of 2. The system is subjected to an external action in the form of slow periodic modulation of an oscillation-controlling parameter and also to an additional action at a frequency that is in an irrational relation with the modulation frequency. It is shown that the variation of the oscillation phase over a modulation period can be approximated by a 2D map on a torus that has a robust (structurally stable) Hunt–Ott strange nonchaotic attractor. Calculations of the quantitative characteristics of the attractor corresponding to the initial set of nonautonomous coupled oscillators (such as phase sensitivity exponent, structures and scaling of rational approximations, as well as Lyapunov exponents and their parameter dependence) confirm the presence of the Hunt–Ott strange nonchaotic attractor.

PACS numbers: 05.45.-a

DOI: 10.1134/S1063784207040020

INTRODUCTION

Nonlinear systems functioning in the presence of a time-variable external action, which are frequently encountered in nature and various fields of technology, are attracting the considerable attention of researchers. Such systems are categorized as nonautonomous. When subjected to even a simple harmonic external action, a nonlinear system may behave in a nontrivial way; for example, periodic oscillations break into chaos or, conversely, chaos is changed to regular motions. If more complex (multifrequency, chaotic, or stochastic) signals are applied to the system, the spectrum of phenomena related to nonlinear nonautonomous dynamics broadens significantly and such effects as chaotic synchronization and stochastic resonance may arise.

Next in ascending order of complexity after the periodic action is the quasi-periodic action, which, in the simplest case, is a superposition of two harmonic signals with an irrational ratio between their frequencies. Quasi-periodically excited systems exhibit specific dynamics associated with the presence of a strange nonchaotic attractor (SNA) in the phase space [1]. Systems with SNAs are nonchaotic in the sense that positive Lyapunov exponents and the exponential instability of phase trajectories in it are absent. However, they show complicated and exotic properties (the fractal geometry of the attractor, singular–continuous spectrum, etc.) [2]. Since 1984, when the SNA was introduced into consideration as a fundamentally new type of the attractor for the first time, this object has been carefully investigated analytically and numerically [3–17] and also experimentally [18–28]. Practical interest in SNAs is related, in particular, to the fact that synchronous systems are viewed as promising for secure data transmission [29, 30].

It should be noted that, in spite of the ample and reliable data concerning the SNA, which were gained in numerical and full-scale experiments, two issues remain open. First, even sophisticated numerical methods proposed to identify the SNA do not assure that the attractor being observed retains a fractal structure on whatever small scales and is really strange, i.e., does not represent a regular, even if very complex, multifrequency regime. Second, SNAs, which are usually observed in the parameter range between quasi-periodic and chaotic dynamics, are highly sensitive to a small variation of the system parameters. Because of the complicated structures of these near-boundary domains, a small change in the control parameters may significantly change the quantitative characteristics of the SNA (such as Lyapunov exponents and indices of phase and parametric sensitivities) and even change the regime qualitatively when the SNA changes to quasi-periodic or chaotic.

In view of the aforesaid, the SNA that has recently been brought into consideration by Hunt and Ott [15, 16] deserves special attention. This attractor is "robust" in the sense that its structure is stable; that is, the fine features of the dynamics are insensitive to any variation of relevant equations and choice of parameter values. It turned out that the existence and the probabi-

listic–metrical properties of such an SNA can be strictly substantiated. It should be emphasized, however, that we are dealing with systems that are described by special iterative maps—artificial models that account for the dynamics in discrete time, with the surface of a 2D torus serving as the phase space. The natural question arises as to whether this type of dynamics can be exemplified in the physical world.

In this work, we consider a system consisting of two coupled nonautonomous van der Pol oscillators that admits of the physical realization of the SNA. An external action appears in the form of a slow periodic modulation of the oscillation-controlling signal in both subsystems in antiphase. This (basic) external action is complemented by an additional one at a frequency that is in irrational relation with the modulation frequency. Based on speculations and numerical results, we show that the dynamics of the variables responsible for the oscillation phase and phase of the additional action over a modulation period are approximated by a map on a 2D torus that falls into the class of Hunt–Ott models demonstrating a robust SNA [15]. Numerical simulations confirm the stability of the attractor against parameter variation: it is observed over a wide domain in the parameter space. The basic dynamic characteristic of any attractor, the Lyapunov maximal nontrivial exponent, turns out to be a smoothly varying function of the system parameters in the domain of existence of the structurally stable SNA. The characteristics of the SNA for the system under consideration that were obtained by the methods reported in [2, 7] are in good agreement with the same characteristics of the attractor in the model map.

HUNT–OTT MODEL

The map suggested by Hunt and Ott has the form [15]

$$\begin{aligned} \varphi_{n+1} &= \varphi_n + \theta_n + \eta F(\varphi_n, \theta_n) (\mathrm{mod} 2\pi), \\ \theta_{n+1} &= \theta_n + 2\pi\omega (\mathrm{mod} 2\pi), \end{aligned} \qquad (1)$$

where $F(\varphi, \theta)$ is a continuous smooth function with a period of 2π in both arguments, η is the nonlinearity parameter, and ω is an irrational parameter characterizing the frequency of a quasi-periodic action.

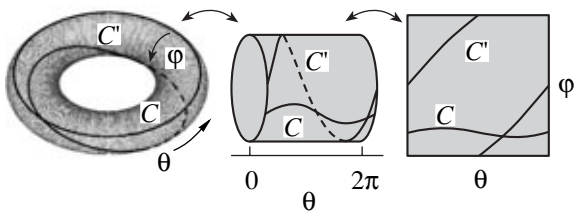

Fig. 1. Schematic representation of the result of single mapping (1) onto a closed curve going round the torus in direction θ.

According to Hunt and Ott's results, when the nonlinearity parameter becomes below critical, $0 < |\eta| < \eta_{cr}$, system (1) exhibits an attractor with the following properties:

(i) the Lyapunov exponent associated with a disturbance of variable φ is negative,

$$\sigma_\varphi = \overline{\lim_{n\to\infty}} (1/n) \sum_{i=1}^{n} \ln\left|1 + \eta F'_\varphi(\varphi_i, \theta_i)\right| < 0; \qquad (2)$$

(ii) the capacitarian and informative dimensions of the attractor are $D_0 = 2$ and $D_1 = 1$, respectively (the difference between these dimensions points to the fractality of the object); and

(iii) the dynamics is structurally stable against small perturbations of system (1) that leave it in the class of systems meeting the above conditions.

According to Hunt and Ott's analysis, the underlying reason for the presence of the robust SNA is the topological character of the map on a 2D torus (Fig. 1): Curve C going round the torus along a parallel is mapped into curve C', which makes one turn along a meridian and one turn along a parallel. After each iteration of the map, the number of turns in the map increases by unity and tends to infinity in the limit of a large number of steps. This introduces fractality into the distribution of the invariant measure over the attractor in the presence of an inhomogeneity due to the nonlinear term in the first of Eqs. (1).

Let us consider an example mapping (1) with nonlinear function $F(\varphi, \theta) = \sin 2\varphi$ (it can be shown in this case that $\eta_c = 0.5$) and irrational frequency parameter $\omega = (\sqrt{5} - 1)/2$ (the inverse golden mean). Figure 2 shows the attractor on the parameter plane (θ, φ) at $\eta = 0.3$, which was obtained after 10^5 iterations of the map. For this example, the Hunt–Ott reasoning is totally applicable, so that we can state with assurance that such behavior is associated with the robust SNA. Owing to the nonlinear term in the first equation, the Lyapunov exponent related to variable φ is other than zero and negative, as it must in the presence of the SNA, $\sigma_\varphi = -0.0242$.

CONSTRUCTION AND QUALITATIVE ANALYSIS OF THE SYSTEM OF COUPLED NONAUTONOMOUS VAN DER POL OSCILLATORS

To construct a physical system where the dynamics of phase variables meets mapping of type (1), let us take two coupled nonautonomous van der Pol oscillators and make use of the idea of relay excitation transfer between subsystems by analogy with [31, 32]. Consider the set of equations

$$\ddot{x} - (A\sin 2\pi t/T - x^2)\dot{x} + (2\pi)^2 x = \varepsilon y \sin[2\pi t + \theta], \qquad (3a)$$

$$\ddot{y} - (-A\sin 2\pi t/T - y^2)\dot{y} + (4\pi)^2 y = \varepsilon x \sin 2\pi t, \quad (3b)$$

$$\dot{\theta} = 2\pi\omega/T, \quad (3c)$$

where x and y characterize the states of the first and second oscillators, respectively, A is the control parameter modulation amplitude, and T is the modulation period.

This set of equations describes a system of two coupled van der Pol oscillators with frequencies $\omega_0 = 2\pi$ and $2\omega_0 = 4\pi$. Due to the modulation of the parameter responsible for the Andronov–Hopf bifurcation, one oscillator operates and the other is below the oscillation threshold over one half-period and vice versa over the next half-period. The first oscillator has an effect on the other through the combinational term that equals the signal of the first oscillator times the reference signal with frequency ω_0. The signal component at double frequency $2\omega_0$ arising in this case serves as a "seed" for the second oscillator when it overcomes the oscillation threshold. The second oscillator, in turn, acts on the first one through the combinational term that is equal to the product of the self-signal and periodic reference signal with a frequency that is in irrational relation with ω_0. This product contains a component at the difference frequency, which is in resonance with the first oscillator and acts as a seed for this oscillator when it starts oscillating. In the normalization adopted, modulation period T is assumed to be an integer number (i.e., it covers an integer number of the periods of the reference signal appearing on the right of the second equation). As for the reference signal on the right of the first equation, it is easy to check that its frequency is $\Omega = 2\pi + 2\pi\omega/T$. From here on, parameter $\omega = (\sqrt{5} - 1)/2$ will be fixed.

Figure 3 shows typical dependences $x(t)$ and $y(t)$ for the operating time of system (3) at $T = 6$, $A = 13$, and $\varepsilon = 0.6$. It can be argued that the variation of the phase variables characterizing system (3) over a modulation period corresponds to a map on the torus of the same topological type as in the Hunt–Ott model. Let us explain this statement in simple terms.

Let the first device start oscillating with initial phase φ,

$$x \sim \sin(2\pi t + \varphi), \quad (4)$$

when the second oscillator is below the oscillation threshold. When the second device starts oscillating, the respective term on the right of Eq. (3b) acts as a seed for self-sustained oscillations appearing in it. This term can be represented as

$$x\sin 2\pi t = \sin(2\pi t + \varphi)\sin 2\pi t$$
$$= (1/2)\cos\varphi - (1/2)\cos(4\pi t + \varphi),$$

where the second term corresponding to the combinational component at the second harmonic, which is in resonance with the second oscillator, seems to dominate. As a result, the second oscillator upon excitation

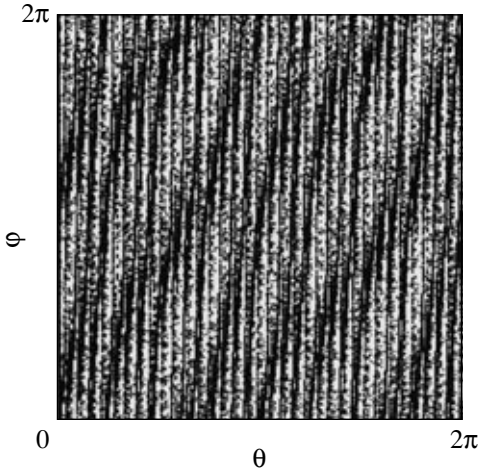

Fig. 2. Phase portrait of the SNA in map (1) for $F(\varphi, \theta) = \sin 2\varphi$, $\omega = (\sqrt{5} - 1)/2$, and $\eta = 0.3$. The number of iterations is 10^5.

Fig. 3. Time variations of variables x and y of system (3) at $T = 6$, $A = 13$, and $\varepsilon = 0.6$ for three modulation periods.

will have phase φ too,

$$y \approx -\cos(4\pi t + \varphi + \kappa_0).$$

Phase correction κ_0 arising when the excitation is transferred from the first oscillator to the second one can be taken to be constant in the crude approximation considered here.

At the next stage of the process, when the first device starts oscillating, the term on the right of the first equation that is represented as

$$y\sin(2\pi t + \theta) = -\cos(4\pi t + \varphi + \kappa_0)\sin(2\pi t + \theta)$$
$$= -\sin(6\pi t + \varphi + \theta + \kappa_0) + \sin(2\pi t + \varphi - \theta + \kappa_0)$$

serves as a seed. Of significance in this sum is the second term, the combinational component at the difference frequency, which falls into the range of resonance frequencies for the first oscillator. As a result, arising oscillations will have the phase

$$\varphi' \approx \varphi - \theta + \nu,$$

which contains phase correction κ_1 due excitation transfer and $\nu = k_0 + \kappa_1$.

Thus, we can conclude that the approximate map of the phase over a modulation period has the form

$$\varphi_{n+1} \approx \varphi_n - \theta_n + \nu (\mathrm{mod}\, 2\pi),$$
$$\theta_{n+1} = \theta_n + 2\pi\omega (\mathrm{mod}\, 2\pi), \quad (5)$$

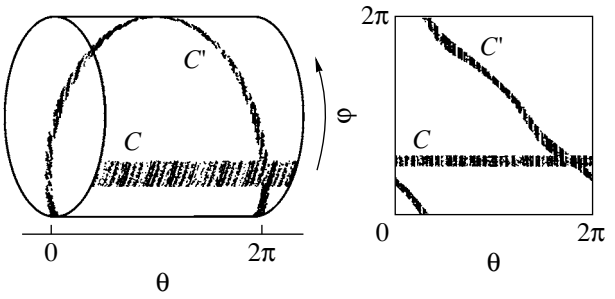

Fig. 4. Numerical illustration of the basic topological property of phase φ in system (3): the band of initial conditions, having gone round the torus in direction θ, acquires an additional turn in direction φ.

which coincides with map (1) at $\eta = 0$ up to substitution ($\phi = 2\pi - \varphi$, $\vartheta = \theta - \nu$).

By numerically solving set of equations (3), one can make sure that the map of the phase evolution of the first oscillator from one excitation stage to another really belongs to the same topological class as the Hunt–Ott model. In the numerical solution, we will determine the phase of the first oscillator at discrete time instants, say, $t_n = n$, using the standard relationships

$$\varphi_n = \begin{cases} \pi/2 - \arctan(\dot{x}(t_n)/2\pi x(t_n)), & x(t_n) > 0 \\ 3\pi/2 - \arctan(\dot{x}(t_n)/2\pi x(t_n)), & x(t_n) < 0. \end{cases} \quad (6)$$

In Fig. 4, the results of analysis of the phase map obtained by numerical calculation at $T = 6$, $A = 13$, and $\varepsilon = 0.6$ are shown graphically. In the robust of computation, phase φ of the first oscillator and its corresponding value of variable θ are sequentially determined at time instants t_n. When φ falls into a certain interval ($\pi/10$ wide), the corresponding dot (θ, φ) is plotted grey and the point meeting the time instant in interval T is plotted black. The curve connecting black dots is mapped into the curve connecting grey dots. As follows from Fig. 4, the topology of these curves meets the assumptions of the Hunt–Ott model: curve C going round the torus along a parallel is mapped into curve C', which makes one turn along a meridian and one turn along a parallel.

Since oscillations produced by van der Pol oscillators are not strictly sinusoidal, the equation for phase φ should be refined by introducing nonlinear term $P(\phi, \theta)$, because of which dissipation appears in the map and an attractor appears in the phase space. Postulating mapping in the form

$$\begin{aligned} \phi_{n+1} &= \phi_n + \theta_n + P(\phi_n, \theta_n) (\mathrm{mod} 2\pi), \\ \theta_{n+1} &= \theta_n + 2\pi\omega (\mathrm{mod} 2\pi), \end{aligned} \quad (7)$$

one can determine function $P(\phi, \theta)$ empirically by numerically solving set of equations (3) under the assumption that this function is smooth and continuous and has a period 2π in either argument. To this end, we proceed as follows. When numerically integrating set (3), we use the data for two successive periods, i.e., for time instants $t_n = n$ $t_{n+1} = n + 1$ to find the quantity

$$P_n = \phi_{n+1} - \phi_n - \theta_n (\mathrm{mod} 2\pi).$$

Then, approximating this function by the 2D Fourier series,

$$P(\phi, \theta) = \sum_{k=-r}^{r} \sum_{m=-r}^{r} [a_{km} \cos(k\phi + m\theta) + b_{km} \sin(k\phi + m\theta)],$$

we determine the coefficients by the least-squares method so as to minimize the residual,

$$\Delta(a_{km}, b_{km}) = \sum_{n=1}^{N} \min_j [P(\phi_n, \theta_n) - (\phi_{n+1} - \phi_n - \theta_n + 2\pi j)]^2.$$

This is achieved by solving the corresponding set of linear algebraic equations in coefficients a_{km} and b_{km}. Calculation was carried out for $T = 6$, $A = 13$, and $\varepsilon = 0.6$. It turns out that the first- and third-order terms of the Fourier series vanish up to a calculation accuracy. With the zeroth- and second-order terms left, the expression for function $P(\phi, \theta)$ has the form

$$\begin{aligned} P(\phi, \theta) \approx &- 1.5578 + 0.1537\cos(2\phi - 0.0351) \\ &- 0.1785\cos(2\theta + 1.4427) \\ &+ 0.1300\cos(2\phi + 2\theta + 0.4251) \\ &- 0.0625\cos(2\phi - 2\theta + 0.2225). \end{aligned}$$

Figure 5 shows the plots of functions $P(\phi, \theta)$ constructed directly from the values P_n, ϕ_n, and θ_n calculated for successive modulation periods in the numerical solution of Eqs. (3) (Fig. 5a) and the plot of function (8) (Fig. 5b). The plots on both panels are in good agreement. Since the dynamics of our system is of the same topological type as the dynamics in the Hunt–Ott model in terms of phase maps, we can infer that a robust SNA is present in out system too.

QUANTITATIVE CHARACTERISTICS OF THE STRUCTURALLY STABLE STRANGE NONCHAOTIC ATTRACTOR

Let us discuss more carefully the approach used to describe the dynamics of couple nonautonomous van der Pol oscillators (see (3)) in terms of maps.

With regard to two phase variables meeting two components of a quasi-periodic external action, the extended phase space can be considered as six-dimensional. Stroboscopically cutting the flow of trajectories in this space at intervals of T, we arrive at a five-dimensional Poincaré map acting in the space of vectors

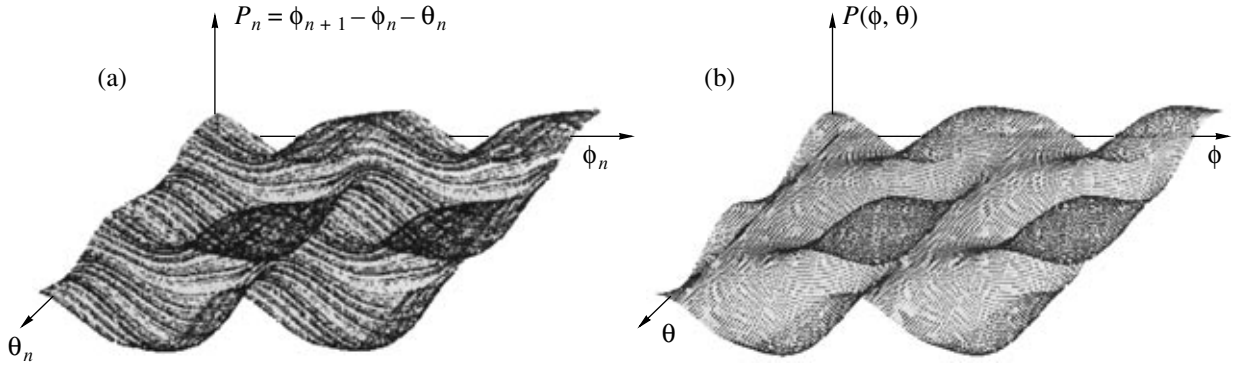

Fig. 5. (a) Set of points (θ_n, ϕ_n, P_n) obtained by direct integration of system (3) and (b) approximation of function $P(\phi, \theta)$ by the Fourier series.

$(x, \dot{x}/2\pi, y, \dot{y}/4\pi, \theta)$. The attractor of this map is characterized by five Lyapunov exponents. One of them is trivial, $\Lambda_0 = 0$, and is related to the disturbances of the phase of angular variable θ. The rest of the exponents, Λ_k $(k = 1–4)$, are negative, as follows from the calculations.

Figure 6a shows the phase portrait of the attractor of the stroboscopic map of system (3) for $T = 6$, $A = 13$, and $\varepsilon = 0.6$. The portrait is shown as the projection onto the plane of variables $(x, \dot{x})$. The portrait of the same attractor on the plane (θ, ϕ) is presented in Fig. 6b. Its obvious visual similarity to the phase portrait of the attractor related to the Hunt–Ott map (Fig. 2) catches the eye. This is because the values of the parameters were consciously taken so as to set in similar regimes in system (3) and map (1) that have, among other things, close leading nontrivial Lyapunov exponents.[1]

To determine nontrivial Lyapunov exponents, set of equations (3) was numerically solved along with four sets of linearized variational equations,

$$\begin{aligned} \delta\ddot{x} + 2x\dot{x}\delta x - (A\sin 2\pi t/T - x^2)\delta\dot{x} + (2\pi)^2\delta x \\ = \varepsilon\delta y\sin[2\pi t(1+\omega/T)], \\ \delta\ddot{y} + 2y\dot{y}\delta y - (-A\sin 2\pi t/T - y^2)\delta\dot{y} + (4\pi)^2\delta y \\ = \varepsilon\delta x\sin 2\pi t, \end{aligned} \tag{8}$$

subject to various initial conditions. Integration was carried out along a trajectory on the attractor within time interval $T \times N$, $N = 10^4$. In every period T, the set of four vectors $(\delta x, \delta\dot{x}/2\pi, \delta y, \delta\dot{y}/4\pi)$ is subjected to the Gram–Schmidt orthogonalization procedure and is normalized to reduce the norms of the vectors to unity. The accumulated sums of the logarithms of the lengths of vectors S_k $(k = 1–4)$ were calculated after orthogonalization but before normalization. The Lyapunov exponents for a map are estimated by the formula $\Lambda_k \cong S_k/N$, and exponents λ_k for system (3) are related with them as $\lambda_k = \Lambda_k/T$. For the dynamics observed at $T = 6$, $A = 13$, and $\varepsilon = 0.6$, the values of the nontrivial Lyapunov exponents are $\lambda_1 \approx -0.0037$, $\lambda_2 \approx -2.74$, $\lambda_3 \approx -2.94$, and $\lambda_4 \approx -2.99$.

The last three exponents are much smaller than λ_1 and are responsible for the fast compression of an elementary phase volume along the directions in the phase space that are transverse to the ϕ axis. It is this fast compression that provides a fairly accurate reduction of the five-dimensional stroboscopic map of system (3) to two-dimensional map (7).

Consider now another quantitative characteristic of the SNA—the phase sensitivity exponent [7], which shows to what extent a typical trajectory on the SNA is sensitive to a change in the initial phase of quasi-periodic force θ. In essence, this exponent is a major attribute of the strange nonchaotic dynamics, since it provides the fractality of the attractor.

For two-dimensional mapping of type (1), the recurrence relation

$$\delta\varphi_{n+1} = \delta\varphi_n[1 + 2\eta\cos 2\varphi_n] + \delta\theta_n, \tag{9}$$

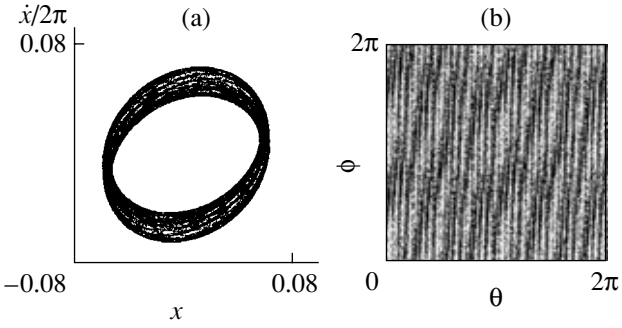

Fig. 6. (a) Projection of the phase portrait of system (3) and (b) phase portrait of empiric map (7) (for the parameter values, see text).

[1] For the regime specified by the above values of the parameters, leading nontrivial Lyapunov exponent $\Lambda_1 \approx -0.0221$ and -0.0242 for system (3) and the attractor of map (1) (Fig. 2), respectively.

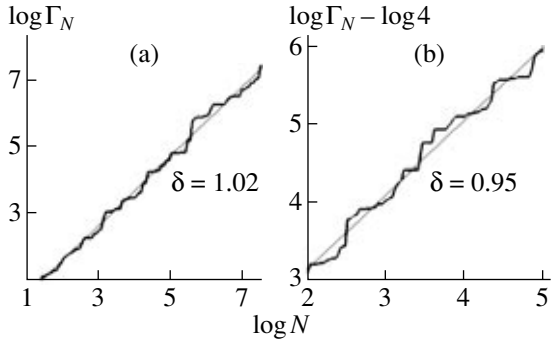

Fig. 7. Phase sensitivity functions calculated for ensembles of 50 trajectories with randomly selected initial conditions for (a) map (1) and (b) system (3).

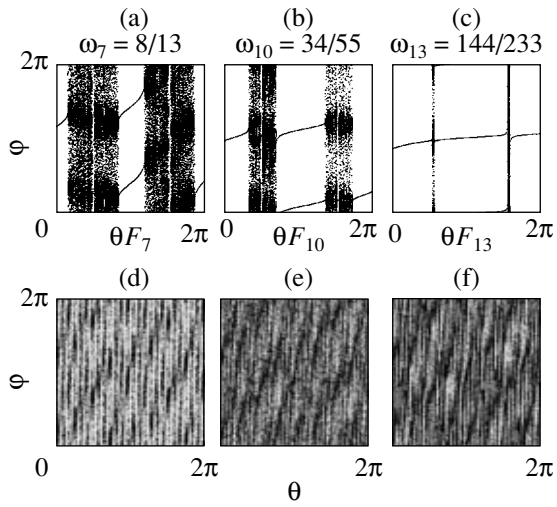

Fig. 8. Approximating sets for the attractor of map (1) at different levels k: (a, d) $\omega_7 = 8/13$, (b, e) $\omega_{10} = 34/55$, and (c, f) $\omega_{13} = 144/233$. The upper row shows the structure of the approximating set within the basic interval $\theta_0 \in [1, 1/F_k)$; the lower row, complete approximation of the attractor at respective level k.

which describes the trajectory disturbance dynamics on the SNA in the presence of small phase deviation $\delta\theta$, is valid. Applying the iteration procedure simultaneously to formula (9) and initial mapping (1), we obtain the values of disturbance $\delta\varphi_n$ at successive instants of discrete time n. Numerical analysis shows that the time dependence of this quantity exhibits high spikes, which grow indefinitely with number of iterations. Following [7], we introduce the phase sensitivity function,

$$\Gamma_N = \min_{\varphi_0,\, \theta_0} \max_{0 \le n \le N} |\delta\varphi_n| \qquad (10)$$

and, assuming that this function increases by a power law at $N \longrightarrow \infty$,

$$\Gamma_N \sim N^{\beta},$$

introduce phase sensitivity exponent β.

To find the same exponent for the system of coupled nonautonomous van der Pol oscillators, we will solve set (3) simultaneously with the set of variational equation

$$\begin{aligned} &\delta\ddot{x} + 2x\dot{x}\delta x - (A\sin 2\pi t/T - x^2)\delta\dot{x} + (2\pi)^2\delta x \\ &= \varepsilon\delta y\sin[2\pi t(1+\omega/T)] + 2\pi\varepsilon y\delta\theta\cos[2\pi t(1+\omega/T)], \\ &\delta\ddot{y} + 2y\dot{y}\delta y - (-A\sin 2\pi t/T - y^2)\delta\dot{y} \\ &+ (4\pi)^2\delta y = \varepsilon\delta x\sin 2\pi t. \end{aligned} \qquad (11)$$

Here, in contrast to relationships (8), constant nonzero variation $\delta\theta$ of the external force phase is specified. The phase sensitivity function can be introduced through the norm of disturbance vector $(\delta x, \delta\dot{x}/2\pi, \delta y, \delta\dot{y}/4\pi)$, $\delta r = \sqrt{(\delta x)^2 + (\delta\dot{x}/2\pi)^2 + (\delta y)^2 + (\delta\dot{y}/4\pi)^2}$; namely,

$$\Gamma_N = \min_{\{x,\, \dot{x},\, y,\, \dot{y},\, \theta\}|t=0} \max_{0 \le t \le NT} \delta r(t). \qquad (12)$$

The log–log plots of the phase sensitivity function versus N for systems (1) and (3) are demonstrated in Fig. 7. The phase sensitivity exponent estimated as the slope of the straight lines approximating these dependences is $\beta \approx 1.02$ for map (1) and ≈ 0.95 for system (3). Within the limits of experimental error (± 0.05), wee can put $\beta = 1$.

The next general characteristic of the attractors of systems (1) and (3) can be found by the method of rational approximations [7]. Let us approximate irrational number ω, the inverse golden mean, by the ratios of Fibonacci numbers, $\omega_k = F_{k-1}/F_k$, where $F_{k+1} = F_k + F_{k-1}$ with $F_0 = 0$ and $F_1 = 1$. At each level k of approximation, the initial quasi-periodically excited system is replaced by an ensemble of systems excited by forces of period F_k that differ in initial phase θ_0. Quantity θ_0 now stands for an additional parameter depending on which a periodically excited system may have a periodic or quasi-periodic attractor. Because of phase periodicity, complete approximation at a kth level is attained by continuously varying initial phase θ_0 within the primary part, $[0, 1/F_k]$, of the phase interval, since the remaining part of the interval, $[1/F_k, 1]$, is covered by $(F_k - 1)$ iterations. The properties of the starting system are reached in the limit $k \longrightarrow \infty$. For finite k, a set of attractors corresponding to different values of phase θ_0 may be viewed as a rational approximation of the attractor of the initial, quasi-periodically excited system.

Figure 8 shows three levels of rational approximation ($k = 7$, 10, and 13) for the attractor of map (1). Each of the patterns is, in essence, a bifurcation diagram for map (1) at $\omega = \omega_k$ where θ_0 serves as a parameter. The ranges of θ_0 corresponding to periodic and aperiodic (more precisely, quasi-periodic, of which one can make certain) regimes can be seen. The latter regimes are represented by "bands" filled with dots. The periodic

regimes are cycles of period mF_k, where m is an integer, which appear and disappear as a result of phase-dependent (i.e., arising in response to θ_0 variation) saddle–node bifurcations. As level k of approximation grows, the part of the phase interval occupied by periodic regimes increases, and the part occupied by quasi-periodic ones narrows.

The attractor of system (3) can be approximated in a similar way. With irrational number ω in Eq. (3c) for phase θ replaced by appropriate rational fractions ω_k, the system can exhibit periodic or quasi-periodic oscillations according to initial phase parameter θ_0. Correspondingly, the form of the attractor of the Poincaré map will also depend on θ_0. At each level of the rational approximation of the attractor, we can construct a bifurcation diagram where initial phase θ_0 stands for a parameter. Figure 9 shows such diagrams for the stroboscopic maps of periodically excited system (3) in the projection onto the plane of variables (θ, ϕ). For convenience of comparison with the diagrams for map (1), the levels of approximation are the same ($k = 7$, 10, and 13). It is seen that the approximating set consists of quasi-periodic regimes and cycles of period mF_k originating from phase-dependent saddle–node bifurcations. As the approximation accuracy is improved, the periodic component dominates and the quasi-periodic one diminishes.

Comparing Figs. 8 and 9, one can see that the structures of the approximating sets for the attractors of map (1) and system (3) qualitatively coincide. The attractors are approximated by quasi-periodic components, main periodic components in the form of cycles with periods F_k and $2F_k$, and narrow intervals of existence of larger period periodic regimes. As level number k (accuracy of approximation) grows, the relevance of the main periodic components of approximation increases, while that of the quasi-periodic components decreases. Let the measures of the periodic and quasi-periodic components of approximation be designated as μ_k and $1 - \mu_k$, respectively. The measures of the quasi-periodic component plotted versus the approximation period are shown in Fig. 10a for map (1) and in Fig. 10b for system (3), respectively. It follows from these figures that the quasi-periodic component decays in both cases by the law $(1 - \mu_k) \sim \exp(-\alpha F_k)$, factors α in the exponents being $\alpha = 0.011$ for map (1) and $\alpha = 0.012$ for system (3) (these values coincide within the limits of regression error).

Thus, it turns out that the quantitative characteristics of the robust SNA of map (1) and SNA of flow system (3) coincide for the parameter values considered. Numerical analysis shows that, when the parameters of system (3) vary insignificantly, the structure of the set approximating the attractor qualitatively remains the same. Phase sensitivity exponent β and factor α entering into the exponent for the rational approximations depend on the parameter values only slightly in the domain of existence of this SNA, which demonstrates the stability of its structure against (at least small) perturbations of the equations in system (3).

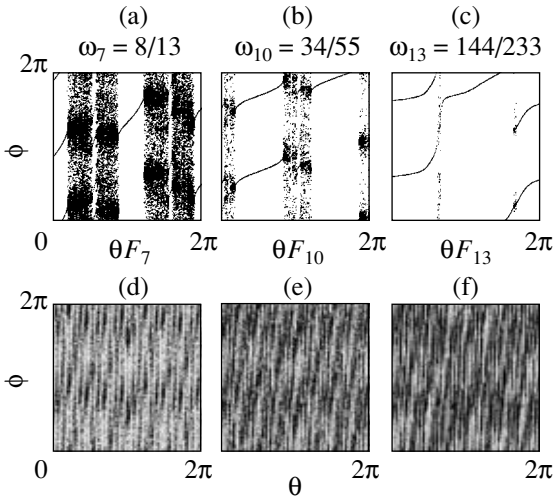

Fig. 9. Rational approximations of the attractor of the stroboscopic map for system (3) in the θ–ϕ coordinates. (a, d) $\omega_7 = 8/13$, (b, e) $\omega_{10} = 34/55$, and (c, f) $\omega_{13} = 144/233$.

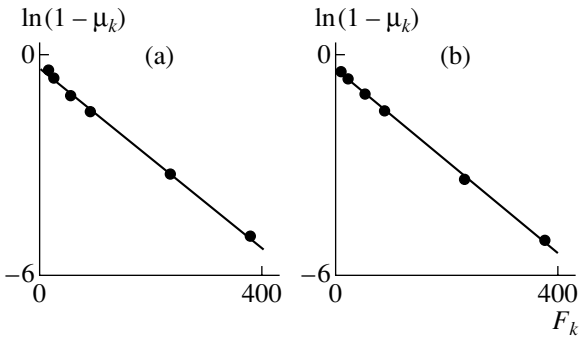

Fig. 10. Measure of the quasi-periodic component in the rational approximation of the attractor vs. level of approximation k for (a) map (1) and (b) system (3).

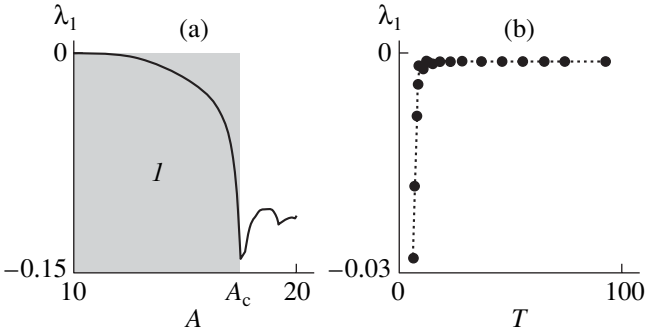

Fig. 11. Leading nontrivial Lyapunov exponent for system (3) vs. the (a) amplitude of modulation of parameter A and (b) modulation period T. (*1*) Robust SNA.

The structurally stable SNA can be observed in a wide range of the parameters of data-flow system (3). Figure 11a illustrates the dependence of leading non-

trivial Lyapunov exponent λ_1 on parameter A (for $T = 6$ and $\varepsilon = 0.6$). The robust (structurally stable) SNA is seen to exist at $A < A_{cr}$. This figure also shows that, after the SNA has originated ($A > A_{cr}$), the A dependence of the Lyapunov exponent becomes smoother. (The remaining Lyapunov exponents of the system vary insignificantly with its parameters.) Figure 11b plots the leading nontrivial Lyapunov exponent versus modulation period T (for $A = 16$ and $\varepsilon = 0.6$). As the period increases (or, in other words, parameter η of map (1) decreases), the exponent tends toward a very small but nonzero steady-state value. In this case, the attractor of the system visually resembles a three-dimensional torus; however, with regard to the Lyapunov exponent spectrum, it should still be considered a strange nonchaotic attractor.

CONCLUSIONS

We for the first time demonstrate the feasibility of nonautonomous dynamics of a new type in a flow system to which a structurally stable strange nonchaotic attractor corresponds. Based on two van der Pol oscillators excited by harmonic signals with irrationally related frequencies, a model system is constructed with the oscillation parameters modulated slowly and in antiphase and with specific coupling providing the relay transfer of the excitation phase. The dynamics of the phase variables characterizing oscillations in the system over the modulation period is approximated by a 2D map on a torus, for which the existence of the robust SNA was rigorously proved by Hunt and Ott. The speculations are confirmed by numerical analysis of the characteristics of the attractor for the constructed system.

It should be emphasized that the system considered in this work obviously admits of a physical implementation based on an electronic device similar to that described in [32].

ACKNOWLEDGMENTS

This work was supported by the Russian Foundation for Basic Research (grant no. 06-02-16619), President of the Russian Federation (grant no. MK-2319.2005.2), and CRDF (grant no. REC-006).

REFERENCES

1. C. Grebogi, E. Ott, S. Pelikan, and J. A. Yorke, Physica D **13**, 261 (1984).
2. S. P. Kuznetsov, A. S. Pikovsky, and U. Feudel, in *Nonlinear Waves*, Ed. by A. V. Gaponov-Grekhov and V. I. Nekorkin (IPF RAN, Nizhni Novgorod, 2005), pp. 484–509 [in Russian].
3. A. Bondeson, E. Ott, and T. M. Antonsen, Phys. Rev. Lett. **55**, 2103 (1985).
4. M. Ding, C. Grebogi, and E. Ott, Phys. Lett. A **137**, 167 (1989).
5. M. Ding, C. Grebogi, and E. Ott, Phys. Rev. A **39**, 2593 (1989).
6. A. S. Pikovsky and U. Feudel, J. Phys. A **27**, 5209 (1994).
7. A. S. Pikovsky and U. Feudel, Chaos **5**, 253 (1995).
8. A. S. Pikovsky, M. A. Zaks, U, Feudel, and J. Kurths, Phys. Rev. E **52**, 285 (1995).
9. U. Feudel, A. S. Pikovsky, and J. Kurths, Physica D **88**, 176 (1995).
10. P. Pokorny, I. Schreiber, and M. Marek, Chaos, Solitons and Fractals **7**, 409 (1996).
11. K. Kaneko and T. Nishikawa, Phys. Rev. E **54**, 6114 (1996).
12. P. Glendinning, Phys. Lett. A **244**, 545 (1998).
13. H. Osinga, J. Wiersig, P. Glendinning, and U. Feudel, Int. J. Bifurcation Chaos Appl. Sci. Eng. **11**, 3085 (2001).
14. A. Prasad, S. S. Negi, and R. Ramaswamy, Int. J. Bifurcation Chaos Appl. Sci. Eng. **11**, 291 (2001).
15. B. R. Hunt and E. Ott, Phys. Rev. Lett. **87**, 254101 (2001).
16. J.-W. Kim, S.-Y. Kim, B. Hunt, and E. Ott, Phys. Rev. E **67**, 036211 (2003).
17. S.-Y. Kim, W. Lim, and E. Ott, Phys. Rev. E **76**, 056203 (2003).
18. W. L. Ditto, M. L. Spano, H. T. Savage, et al., Phys. Rev. Lett. **65**, 533 (1990).
19. S. T. Vohra, F. Bucholtz, K. P. Koo, and D. M. Dagenais, Phys. Rev. Lett. **66**, 212 (1991).
20. T. Zhou, F. Moss, and A. Bulsara, Phys. Rev. A **45**, 5394 (1992).
21. K.-P. Zeyer, A. F. Miinster, and F. W. Schneider, J. Phys. Chem. **99**, 13373 (1995).
22. W. X. Ding, H. Deutsch, A. Dinklage, and C. Wilke, Phys. Rev. E **55**, 3769 (1997).
23. T. Yang and K. Bilimgut, Phys. Lett. A **236**, 494 (1997).
24. Y. H. Yu, D. C. Kim, J. Y. Ryu, and S. R. Hong, J. Korean Phys. Soc. **34**, 130 (1999).
25. B. P. Bezruchko, S. P. Kuznetsov, and Y. P. Seleznev, Phys. Rev. E **62**, 7287 (2000).
26. D. Sanchez, G. Platero, and L. L. Bonilla, Phys. Rev. B **63**, 201306 (2001).
27. A. Vaszlenko and O. Feely, Int. J. Bifurcation Chaos Appl. Sci. Eng. **12**, 1633 (2002).
28. E. P. Seleznev and A. M. Zakharevich, Pis'ma Zh. Tekh. Fiz. **31** (17), 13 (2005) [Tech. Phys. Lett. **31**, 725 (2005)].
29. R. Ramaswamy, Phys. Rev. E **56**, 7294 (1997).
30. C. Zhou and T. Chen, Europhys. Lett. **38**, 261 (1997).
31. S. P. Kuznetsov, Phys. Rev. Lett. **95**, 144101 (2005).
32. S. P. Kuznetsov and E. P. Seleznev, Zh. Éksp. Teor. Fiz. **129**, 400 (2006) [JETP **102**, 355 (2006)].

Translated by V. Isaakyan